Int. J. Multiphase Flow, Vol. 2, pp. 235–246. Pergamon/Elsevier, 1975. Printed in Great Britain.

TURBULENCE STRUCTURE OF AIR–WATER BUBBLY FLOW—II. LOCAL PROPERTIES

AKIMI SERIZAWA

Institute of Atomic Energy, Kyoto University, Uji, Kyoto, Japan

and

ISAO KATAOKA and ITARU MICHIYOSHI

Department of Nuclear Engineering, Kyoto University, Sakyo-ku, Kyoto, Japan

(*Received* 1 *September* 1974)

Abstract—Microstructure was studied experimentally in air–water two-phase bubbly flow flowing upward in a vertical pipe of 60 mm diameter under atmospheric pressure. The results indicate that over a large portion of fully-developed bubbly flow the phases, the velocities of bubbles and water, and the ratio between the velocities of the phases have fairly flat radial profiles. In the wall region a maximum void fraction was observed. Spectra of the velocities of bubbles and water showed a Poisson distribution and a normal distribution function, respectively. The experimental evidence indicated a trend for the turbulent intensity to decrease first with increasing gas flow rate for constant water velocity and to increase again with a further increase in the gas flow rate. This phenomenon was more significant for a higher water velocity.

INTRODUCTION

Bubbles suspended in liquid undergo various phenomena too complex for mathematical formulation. Complicated interactions like collisions and coalescences between adjacent bubbles, interactions between bubbles and the pipe wall, and transfiguration of bubbles affect the local conditions of the flow field, causing fluctuations in static pressure and in velocity, violent turbulent motion of the liquid etc. The resultant variation of the flow field induces the change of bubble motion, and this may result ultimately in either more violent fluctuation or heterogeneity of the flow. Much effort has been spent analytically (Brandt 1958; van Deemter 1961; Vohr 1962; Lamb & White 1962; Levy 1963; Brown & Kranich 1968), but such models cannot represent the flow situation as it actually exists and can be applied only to well-defined or strictly limited flow conditions.

On the other hand, though a relatively large amount of experimental work has been performed as to the structure of bubbly flow with many different gas–liquid systems, comparisons of the results of many studies provide little in the way of common basic information which presents an insight into the physical phenomena. This follows partly from the fact that such studies were confined to the measurements of only one or two parameters under different flow conditions, and partly from the perplexing statistical nature of the random fluid motions induced by bubbles moving in random manner. Thus, even the basic knowledge about the mechanism of this complex flow is still very limited, although gas bubbles in liquid are a very familiar sight.

The most significant and essential parameters associated with this flow pattern are the distribution of gas and liquid phases, the bubble velocity and its spectrum, the liquid velocity and its fluctuating terms, the bubble size distribution, the bubble transit frequency, the rates of turbulent diffusion of mass, momentum or heat, shear stress *etc.* These variables are able to describe the local flow conditions of the steady-state bubbly flow, both qualitatively and quantitatively. Hence, accurate information about such flow variables and the generalized relationships among them are quite necessary to understand the turbulent transport phenomena of two-phase bubbly flow as they actually exist.

The present work is an experimental study of various local parameters and some of the

turbulence characteristics of cocurrent air–water two-phase bubbly flow, flowing upward in a vertical circular tube of 60 mm i.d. under nearly atmospheric pressure. Emphases are put on the following:

(1) Measurment of the local parameters.
(2) Clarification of the entrance effect upon the flow.
(3) Description of some statistical characteristics of air–water flow.
(4) Obtaining the basic information about the turbulent transport process in air–water bubbly flow.
(5) Finding generalized correlations among those parameters.
(6) Development of an appropriate model based upon a diffusive nature of bubbles suspended in turbulent flow.

EXPERIMENTAL APPARATUS AND PROCEDURE

A schematic diagram of the experimental facility is presented in figure 1. The 2100-mm long vertical smooth test section is divided into three parts which are made of 60 mm inside diameter Lucite tubing. A Lucite chamber with mounting studs for probe equipment was used for the convenience of probe installation. A 220-mm long Lucite calming section was used between the mixer and the test section, whose upstream inside diameter was 104 mm and the downstream inside diameter 60 mm. Air entered through the 17·5 mm i.d. pipe at the bottom of the mixer and merged with the water stream through a series of 84 holes of 1·5 mm diameter, spaced along the periphery of the 42·7 mm o.d. pipe. A 150-mesh stainless steel screen was placed as a bubble diffuser between the mixer and the calming section.

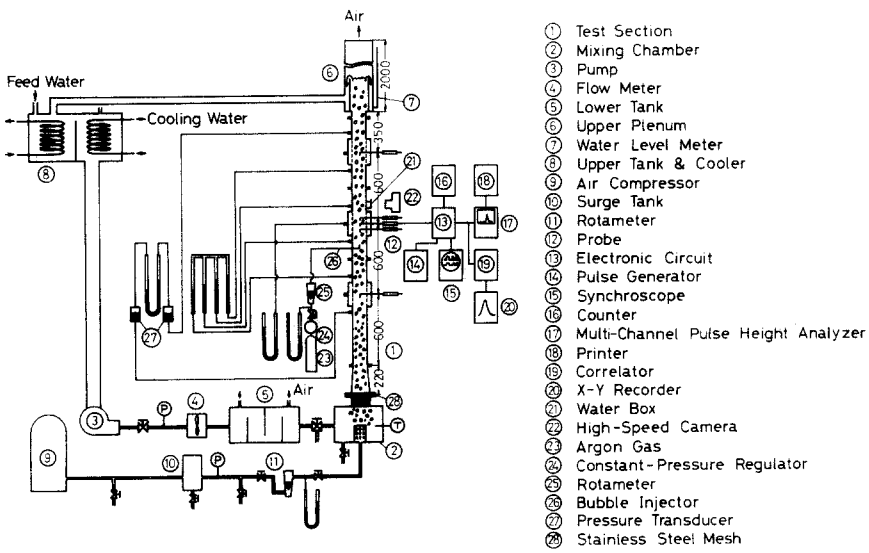

Figure 1. Schematic diagram of experimental facility.

Tap-water was circulated from the upper tank through the loop by means of a pump, being degassed at the lower plenum. The water flow was controlled by a valve and measured by a turbine flowmeter. The air flow was measured by means of a rotameter. The metered streams of air and water were fed to the bottom of the test section, and the resulting two-phase mixture flowed up through the test section and into the separator where the air was liberated to the atmosphere.

Measurements were performed at three axial positions, $Z/D = 10$, 20 and 30. The probes were radially traversed every 1 or 2 mm from $r/R = -0{\cdot}98$ to $+0{\cdot}98$ ($r/R = +1{\cdot}0$ and $-1{\cdot}0$ represent the positions on the inner surface of the pipe on either side of the mounting studs for probes, respectively). The ranges of the flow variables covered in this experimental study were: superficial water velocity $V_0 = 0{\cdot}30$ to $1{\cdot}03$ m/sec, quality $X = 0{\cdot}0085$ to $0{\cdot}0900$ per cent, water temperature $T_1 = 291$ to 295°K, system pressure $P \simeq 0{\cdot}11$ MPa absolute, and mean bubble diameter $\bar{d} \simeq 4$ mm.

EXPERIMENTAL RESULTS AND DISCUSSIONS

Flow pattern map

Flow patterns were determined both by visual observation and by recorded signals of three resistivity probes located at the pipe center at $Z/D = 10$, 20 and 30. Three types of flow patterns were defined, i.e. bubbly flow, bubble-to-slug transition flow, and slug flow. Figure 2 shows the flow pattern map in the form of the superficial water velocity vs quality diagram.

Entrance effects on development of two-phase flow

To provide sufficient information to evaluate the effects of a sudden geometry change of flow area, or of the entrance effect on two-phase flow development (needed for a detailed inspection of the experimental results) measurements of axially changing profiles of the local void fraction, local mean bubble velocity, and the standard deviation of the bubble velocity spectrum were performed at three axial positions, $Z/D = 10$, 20 and 30.

Typical results are presented in figure 3, showing void fraction and bubble velocity profiles measured by a cross-correlation technique. It can be seen from this figure that the profiles of the local void fraction and local mean bubble velocity are clearly changing as the flow enters the test section, and that the axial symmetry in both profiles is very poor at $Z/D = 10$, comparatively good at $Z/D = 20$, and is reasonably satisfied at $Z/D = 30$. The results of the relative standard deviation of bubble velocity spectrum are demonstrated in figure 4. It should be noted that in the bubbly flow region the relative standard deviation is nearly uniform across the tube ($s/V_b = 0{\cdot}1$ to $0{\cdot}2$) and is smaller for a larger downstream distance. In transition and slug flows, the results indicate a larger value ($s/V_b = 0{\cdot}2$ to $0{\cdot}3$) than in bubbly flow, with a trend to larger values in the core region of the flow and smaller values in the wall proximity. However, its profile does not present a further significant axial change.

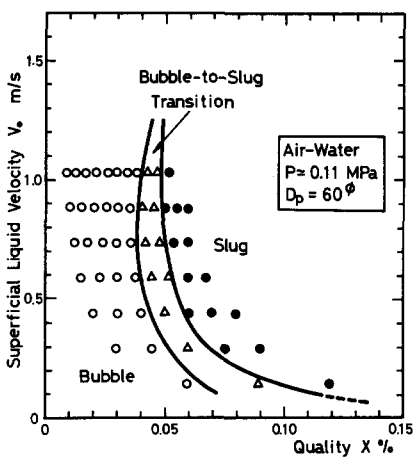

Figure 2. Flow pattern map.

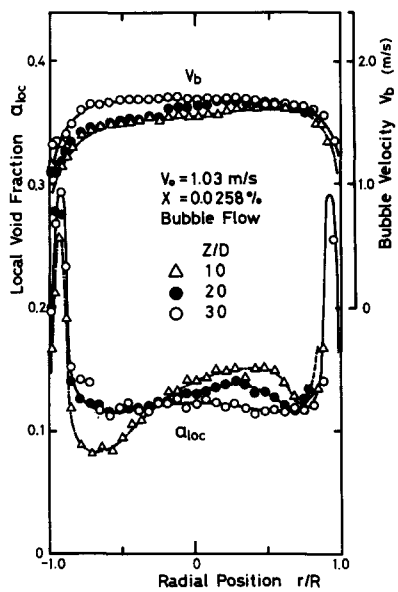

Figure 3. Entrance effect upon flow arrangement.

All these experimental trends reveal that nearly fully-developed flow is already attained at $Z/D = 30$ for bubbly flow, whereas in transition and slug flows, the entrance length is less than $30D$. This is perhaps because in bubbly flow, the flow perturbation occurring at the entrance to the test section overcomes the intrinsic turbulent characteristics of the flow. On the other hand, in both transition and slug flows, violent mixing actions of the flow may precipitate the flow arrangement.

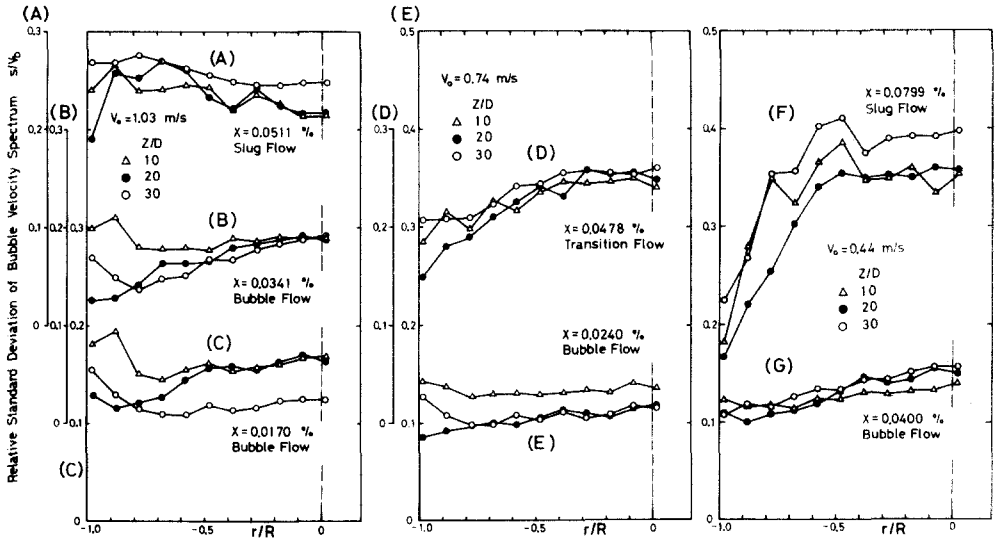

Figure 4. Entrance effect upon flow arrangement.

Profiles of void fraction and bubble impaction rate

The local void fraction and bubble impaction rate were measured by means of a void probe at the upper part of the test section, $Z/D = 30$, where fully-developed flow was already established.

Examples of the local void fraction distribution obtained are shown in figure 5. They show that the distribution of the void fraction is a strong function of the flow pattern and changes from a saddle shaped distribution to a parabolic-shape as the gas flow or the quality increases at constant water velocity. A saddle shape distribution corresponds to bubbly flow, and a parabolic-shape distribution to slug flow. The peaking phenomenon of the local void fraction was observed in the vicinity of the pipe wall commonly in the low quality region. The effect of increasing quality at constant water velocity is to decrease the peak value of the void fraction near the wall relative to the value at the pipe center. This peak exists at the position away from the wall by a distance of nearly one mean bubble radius. A similar trend in the void fraction profile has been reported by many other investigators for air–water (Malnes 1966; Kobayashi *et al.* 1969; Aoki *et al.* 1969; Sekoguchi *et al.* 1972), steam–water (Kazin 1964), and gas–mercury flow (Neal 1963; Tamao 1970).

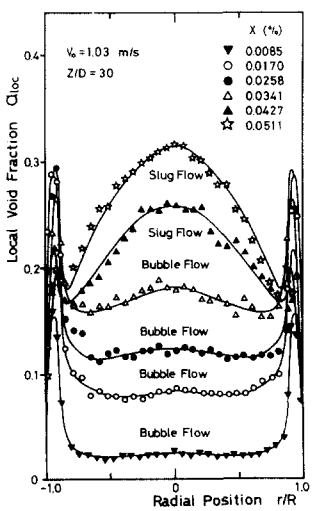

Figure 5. Void fraction profiles.

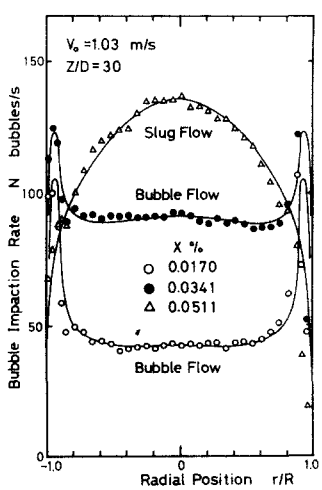

Figure 6. Bubble impaction rate profiles.

Typical bubble number distributions are presented in figure 6 in terms of bubble impaction rate. Similarly to the void fraction distribution, the bubble number distribution is saddle shaped in bubbly flow, whereas it is parabolic-shaped in slug flow. The peaking phenomenon near the wall was also observed corresponding to that in the void fraction distribution. This bubble trapping is mainly due to the effects of the hydrodynamic forces acting on a bubble such as the Magnus force and Zhukovski force, and partly due to the interactions between bubbles and the wall, such as adherence or reflection of bubbles at the surface of the wall. These hydrodynamic forces and the wall effects must be studied further (Rouhani 1974).

Bubble velocity and its spectrum

The bubble velocity spectrum was measured using a double sensor probe by multichannel technique. The measuring time interval was 3 to 20 min according to the number of bubbles passing over the measuring station, giving the results a statistical meaning. Typical spectra obtained at the pipe center are given in figure 7 for several qualities. Solid lines drawn for each spectrum represent Poisson distribution functions fitted to each spectrum (Petrick 1962). These representations indicate that the bubble velocity spectrum at the pipe center can be well approximated by a Poisson distribution for bubbly flow, while for slug flow it tends to deviate from that distribution due to the slugs flowing at higher velocities than smaller bubbles. In bubbly flow the shape of the spectrum did not change significantly either along the flow direction or in the radial direction.

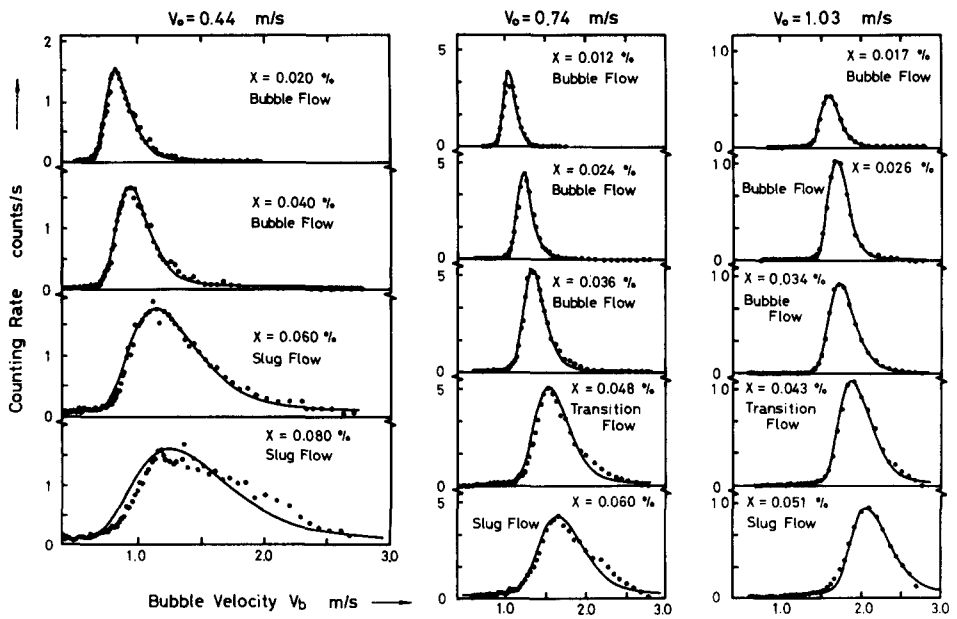

Figure 7. Bubble velocity spectrum (at $r/R = 0$).

The local mean bubble velocity was calculated from the bubble velocity spectrum according to [4] in the previous paper, and are presented in figure 8. From this figure, it may be concluded that the bubble velocity distribution can be approximated by the power law expression similar to the normal turbulent velocity profile.

Also from figure 8, the relative standard deviation of the bubble velocity spectrum shows a fairly uniform distribution over a large portion of the flow area, except for the wall region. In bubbly flow, the value s/V_b generally increases with increasing quality for constant flow rate of water. This is partly due to a change in the mixing actions of the liquid caused by more densely concentrated bubbles (the turbulent intensity of the flow does not necessarily increase linearly with an increase in quality, figure 12), and is partly due to the more effective interactions between bubbles. The effect of increasing water velocity for constant quality is to decrease the bubble

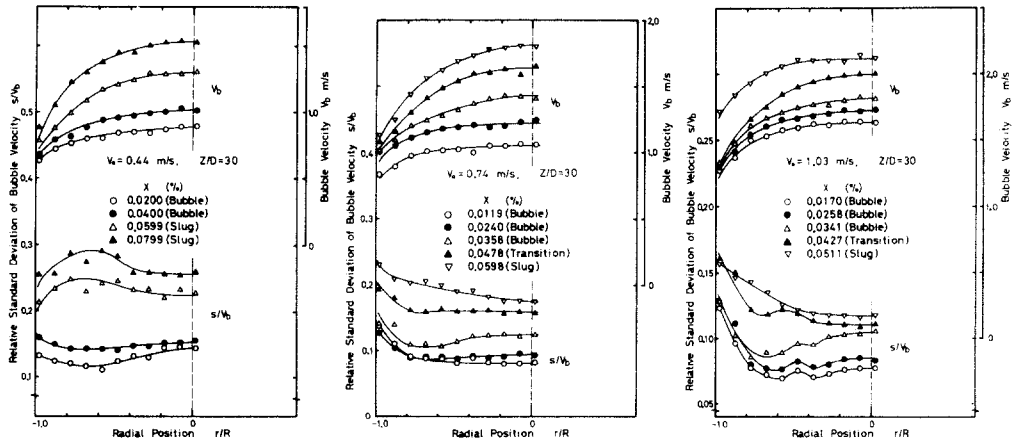

Figure 8. Bubble velocity and its relative standard deviation.

velocity fluctuation. This may be explained as follows. As the water velocity is increased, the fluctuating motions of bubbles suspended in the stream become relatively suppressed by the intensified inertial force of the water (in the present experiment, the bubble size did not vary significantly with a change in water velocity).

The local relative velocity of bubbles $V_s(r)$ and the local velocity ratio $S_{loc}(r)$ are defined, using ensemble-average local mean bubble velocity $V_b(r)$ and time-average liquid velocity $V_l(r)$:

$$V_s(r) = V_b(r) - V_l(r), \qquad [1]$$

$$S_{loc}(r) = V_b(r)/V_l(r). \qquad [2]$$

Typical results are represented in figure 9. In bubbly flow the result shows nearly uniform distributions of the velocity ratio (the so-called slip ratio) and the inflated distribution of the relative velocity. As the quality increases at constant water velocity, the relative velocity generally increases and its profile becomes sharper. An effect of the flow pattern upon the relative velocity seems to exist, but details could not be clarified.

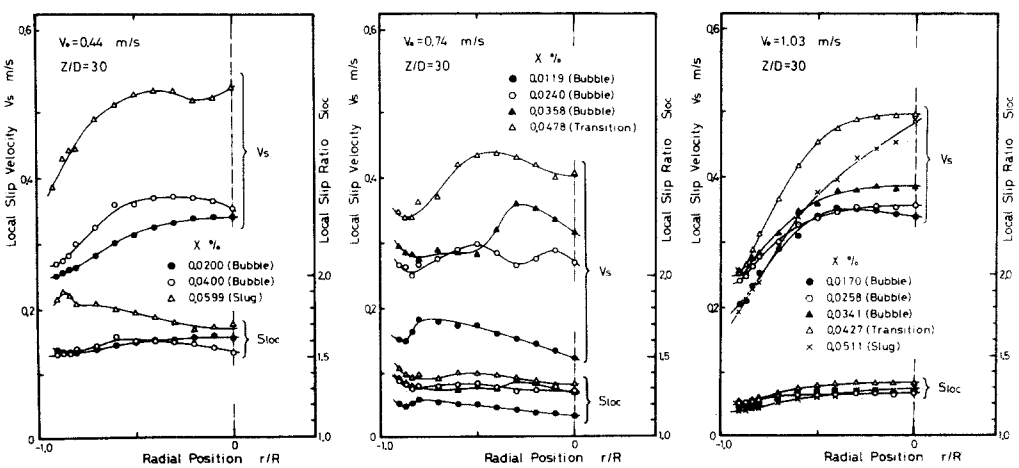

Figure 9. Local relative velocity and local slip ratio.

Water velocity and its spectrum

The liquid velocity profile plays a decisively important role in characterizing the flow structure. Such information is definitely required for two-phase flow investigation. Following Delhaye (1969)

using a hot-film anemometer and a 400-channel analyzer, the profiles of the water velocity and the corresponding longitudinal turbulent intensity were measured.

Typical water velocity spectra are given in figure 10 for several radial positions. By taking account of the additional background component due to bubble passages (see the previous paper), it may be realized from this figure that the water velocity spectrum can be well approximated by a normal distribution function. This fact, coupled with a Poisson distribution of the bubble velocity spectrum, implies that the water velocity fluctuates independently of the velocity of the leading or the following bubbles whose momentum is sufficiently small.

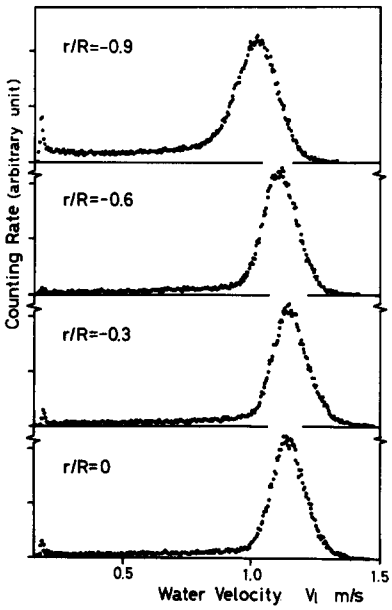

Figure 10. Water velocity spectrum. (Bubbly flow: $V_0 = 0{\cdot}88$ m/sec, $X = 0{\cdot}0300\%$, $Z/D = 30$.)

Figure 11 shows the water velocity profiles deduced from the water velocity spectrum. As the quality is increased in the low bubble density and high water flow rate region from zero up to below a certain value determined by water flow rate, the water velocity profile changes from the normal turbulent velocity profile, i.e. 1/7-power law, to a plug-shaped profile (nearly uniform distribution). The water velocity near the pipe axis is sometimes lower than in single-phase water flow. The dominant flow pattern in this quality range is bubbly flow of lower void fraction. When the gas flow is significantly increased, the profile changes from a flat distribution to a dome-shaped one with a maximum at the pipe center. Concurrent with this change, the flow pattern changes from bubbly flow to slug flow. No significant peaking near the wall was observed in any experimental run. The flat profile of the water velocity is perhaps due to the acceleration effect of more densely concentrated bubbles near the wall.

Profiles of the relative turbulent intensity $I_1 (= \sqrt{\overline{u^2}}/V_1)$ are shown also in figure 11. The value I_1 generally increases toward the wall and has a minimum at the pipe center. In bubbly flow a uniform distribution of the relative turbulent intensity was observed, especially for a higher superficial water velocity.

Profiles of the longitudinal turbulent velocity $\sqrt{\overline{u^2}}$ are indicated in figure 12. In bubbly flow of lower void fraction, the turbulent velocity also distributes uniformly, and it exhibits, in some cases of higher water velocity, somewhat lower values than those obtained in single-phase water flow. This is an interesting phenomenon which is contrary to our intuition that the flow should be more strongly disordered by introducing the agitating bubbles into the stream. A similar effect upon the turbulent intensity or its energy spectrum by introducing solid particles of small size into a liquid stream has been reported in detail by Hino (1967). This phenomenon in bubbly flow may be ascribed to the competition among the following effects and others:

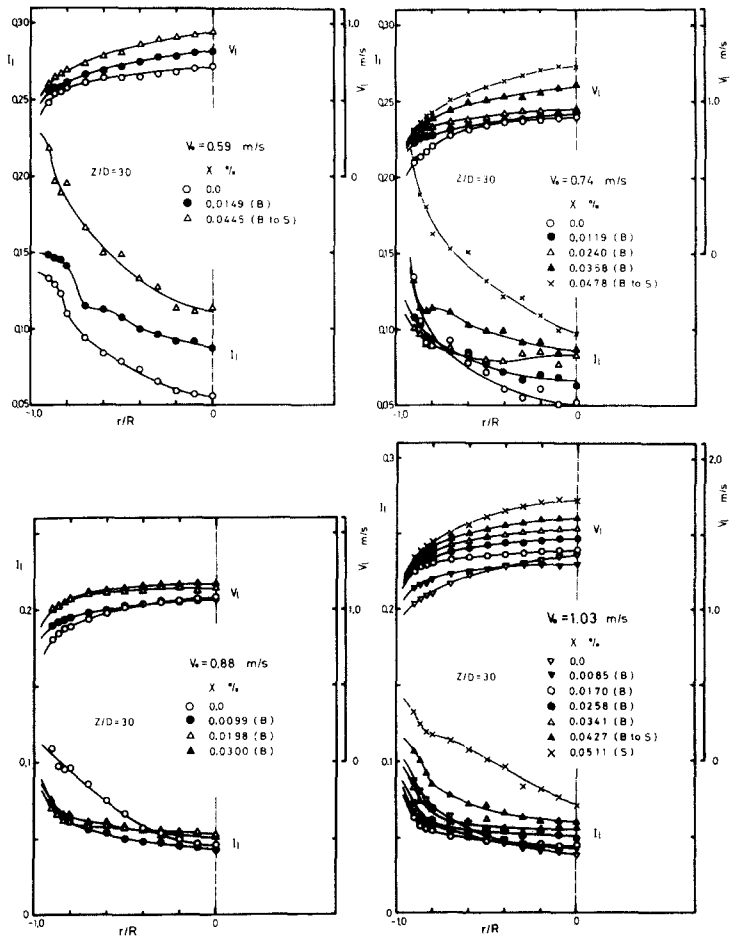

Figure 11. Water velocity and relative turbulent intensity.

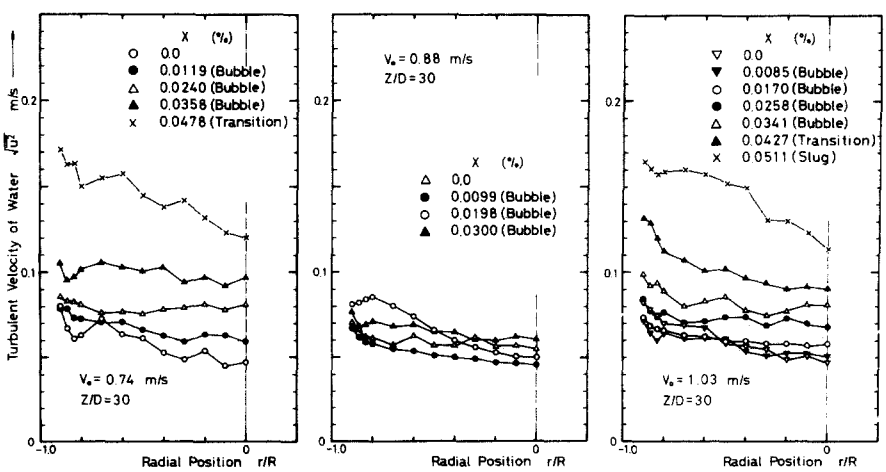

Figure 12. Longitudinal turbulent velocity of water.

(1) Decrease in the effective volume of the liquid phase for energy dissipation due to the volume occupied by the suspended bubbles—this effect is to increase the turbulent intensity.

(2) Work done for floating the bubbles—this effect serves to reduce the turbulent intensity.

(3) Energy dissipation associated with the lateral relative motions or rotations of bubbles—the turbulent intensity may be decreased in order to supply this energy dissipation.

(4) An energy-absorbing character of bubbles—bubbles may act as a kind of energy absorber. The turbulent energy obtained from the liquid may be dissipated by the circulating motions of the gas within bubbles or by the hydrodynamic motions of bubbles other than those described in (2) and (3). Many corrugations of various shapes observed on the surface of every bubble, as seen in figure 16, appear to verify this argument.

Hino suggested that the elongation of the mixing length might follow a decrease in energy production at constant radius. However, figure 13 cannot give any direct experimental verification to the validity of his argument. (This mixing length shown in figure 13 was evaluated by employing a mixing length concept, and τ is the shear stress. Details should be referred to the following paper.) More detailed and pertinent studies are strongly needed for more accurate and realistic interpretation of this phenomenon.

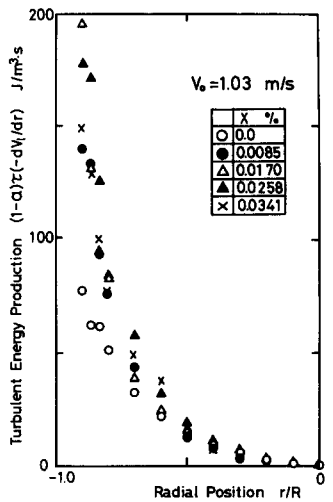

Figure 13. (a) Turbulent energy production in bubbly flow.

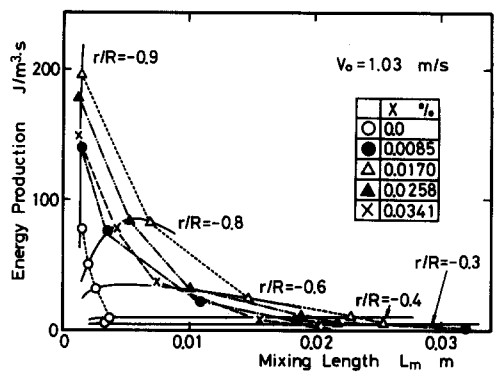

Figure 13. (b) Turbulent energy production vs mixing length.

Empirical relationships between variables

In the foregoing paragraphs, the important variables specifying an air–water two-phase bubbly flow have been discussed individually. All these variables affect each other in a very complicated fashion. To draw any general conclusions it is necessary to obtain a sound insight of the physical picture of the flow mechanism.

Figure 14 gives correlative representations of the empirical relationships among local parameters. As seen from this figure, in bubbly flow the radial variations of all the representative parameters are uniform over the central core region of $|r/R| < 0{\cdot}7$ to $0{\cdot}8$, where the turbulent transport in the radial direction is evaluated to be overwhelmingly predominant due to the continuous stirring effects of small bubbles. In the outer region of the flow where direct viscous effects are still negligibly small, almost all parameters either increase or decrease rapidly with radius because of the wall effects.

Some statistical properties of bubble behavior

A study of the statistical nature of bubble motion is also required from a viewpoint of a bubble diffusion model. Here, we discuss briefly the experimental results of the Eulerian auto-correlation function of the phase change detected by the void probe, bubble size distribution, and the distribution of the time interval between bubble transits or bubble impingements on the void probe.

In the bubbly flow region, the auto-correlation function of the phase change decreased nearly exponentially with time lag independently of the position of the probe in the stream. In transition and slug flows, the periodic occurrence of slugs deviates this function from an exponential shape, and the function incurs naturally an increase at large values of time lag. This characteristic deviation of the function may serve as a means for distinguishing bubbly flow from others.

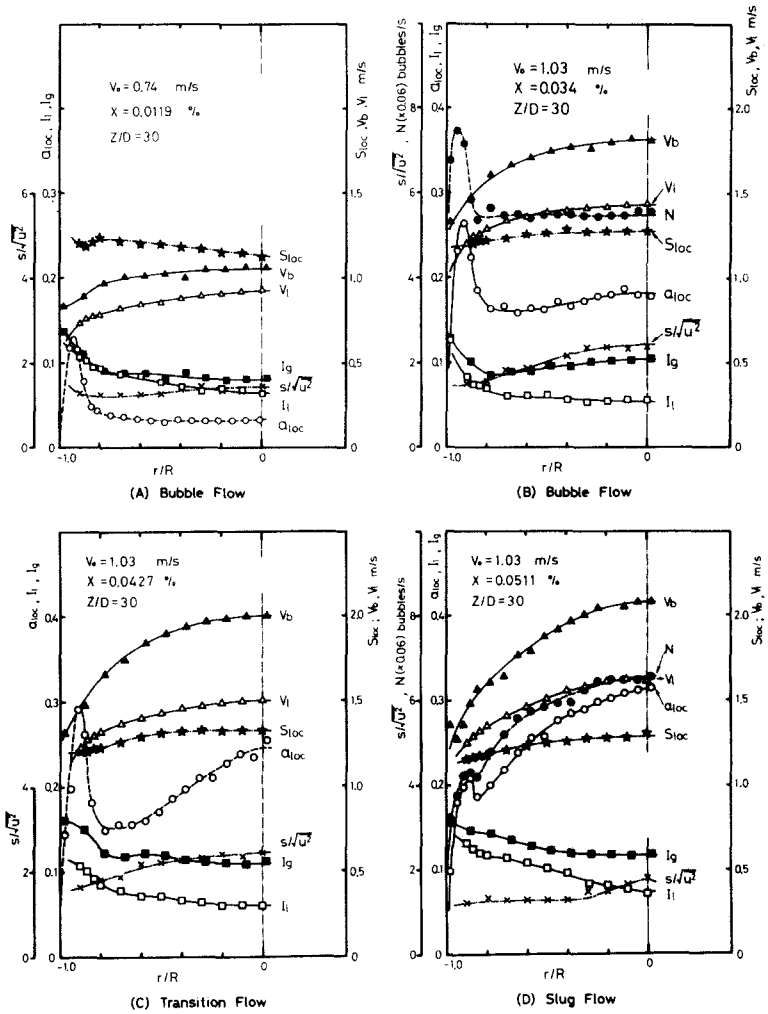

Figure 14. Correlative representations of various local parameters.

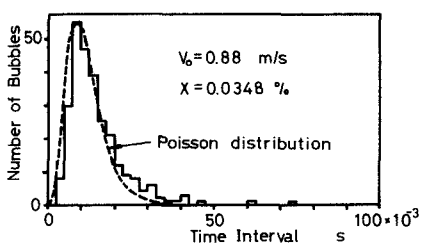

Figure 15. Histogram of time interval between bubble impingements on void probe.

Figure 15 indicates a typical histogram of the time interval between bubble impingements on the void probe. From this figure, it is realized that the temporal distribution of the bubble transit in bubbly flow is well approximated by a Poisson distribution function (broken line in the figure).

The equivalent-spherical-diameter of bubbles was obtained from bubble photographs with a planimeter. The resulting bubble size distribution presented a trend similar to a normal distribution function. In all experimental runs in bubbly flow, the mean bubble size was between 3·5 to 4 mm in equivalent-spherical diameter, regardless of the water velocity and the quality.

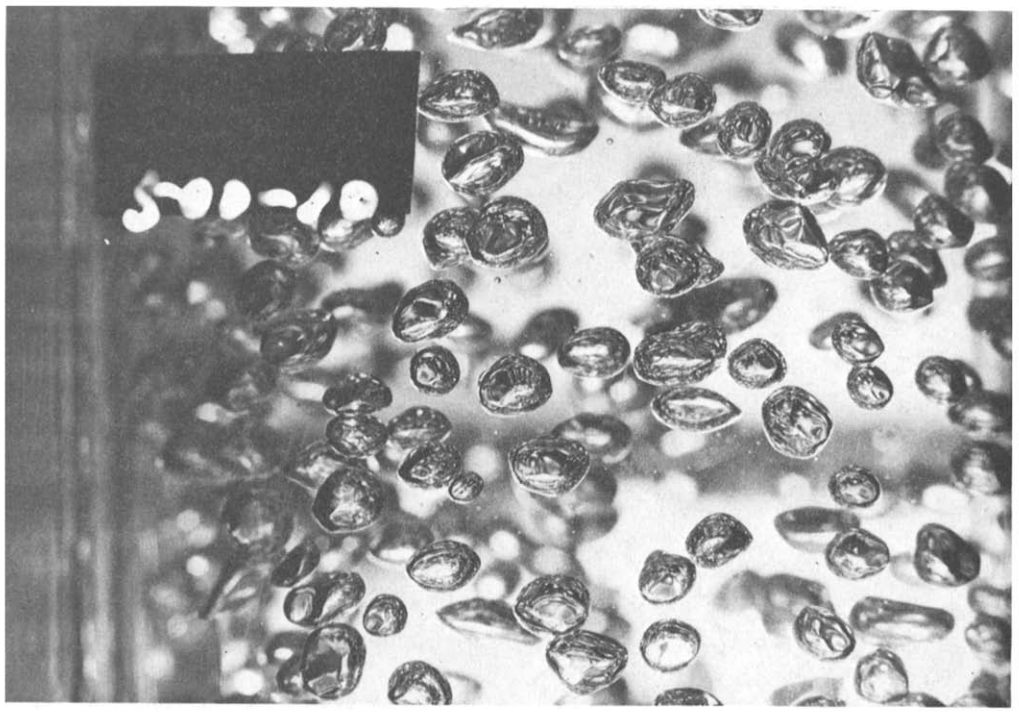

Figure 16. Typical bubble photograph. (Bubbly flow: $V_0 = 0{\cdot}74$ m/sec, $X = 0{\cdot}0119\%$, $Z/D = 22{\cdot}5$).

CONCLUSIONS

A considerable amount of information has been obtained on the turbulence structure of air–water two-phase bubbly flow in a pipe, which gives a correct physical picture of the flow.

The experimental results indicate that over a large portion of any cross section in fully-developed bubbly flow region, most of the various local parameters are uniformly distributed in the radial direction. This may support the validity for applying a homogeneous flow field to an air–water bubbly flow of small quality. Uniform distributions of the local parameters follow from the intensified turbulent transport of the transferable quantities. On the other hand, in the outer (wall) region of the flow, wall effects appear in maxima of the local void fraction and bubble impaction rate. These wall effects need to be studied in further detail.

The statistical character of bubble rise velocity and the water velocity was studied. Spectra of the bubble velocity and the water velocity showed a Poisson distribution and a normal distribution function, respectively. A particularly important and interesting phenomenon was found for the turbulent intensity. The experimental evidence indicated a trend for the longitudinal turbulent intensity to decrease with increasing gas flow rate for constant water velocity, and then increase with a further increase in the gas flow rate. This phenomenon was stronger for a higher water velocity. However, this peculiar phenomenon could not be satisfactorily clarified; the corrugated surface of bubbles observed by photographs gives some useful suggestions to aid in understanding the physical picture of flow turbulence in gas–liquid two-phase bubbly flow.

Additional data on the entrance effects upon the flow arrangement, Eulerian auto-correlation function of the phase change, time interval between bubble impingements on the void probe, and bubble size are also obtained and summarized.

REFERENCES

AOKI, S., INOUE, A. & YAEGASHI, H. 1969 The local void fraction and velocities of the phases in two-phase bubbly flow in a vertical tube. *Proc. 6th Japan. Heat Trans. Symp.* pp. 241–244.

BRANDT, F. 1958 Der reibungsdruckverlust von wasser-damfgemischen und die voreilgeschwindigkeit des dampfes gegenüber dem wasser in senkrechten kesselrohren. Dissertation, Darmstadt.

BROWN, F. C. & KRANICH, W. L. 1968 A model for the prediction of velocity and void fraction profiles in two-phase flow, *A.I.Ch.E. Jl* **14**, 750–758.

DELHAYE, J. M. 1969 Hot-film anemometry in two-phase flow. *Proc. 11th Nat. ASME/AIChE Heat Transfer Conf. on Two-Phase Flow Instrumentation*, Minneapolis, Minnesota. pp. 58–69.

HINO, M. 1967 Micro-structure of solid-liquid two-phase flow. *Proc. Symp. on Multi-Phase Mixture.* Prepared by Sci. Council of Japan. pp. 21–30.

KAZIN, I. V. 1964 Radial distribution of steam in a rising turbulent steam–water flow, *Teploenergetika* **11**, 40–43.

KOBAYASHI, K., IIDA, Y. & KANEGAE, N. 1969 Local void fraction profiles in gas/liquid two-phase flow in vertical tubes, *Trans. Japan. Soc. Mech. Engrs* **35**, 2365–2372.

LAMB, D. E. & WHITE, J. L. 1962 Use of momentum and energy equations in two-phase flow, *A.I.Ch.E. Jl* **8**, 281–283.

LEVY, S. 1963 Prediction of two-phase pressure drop and density distribution from mixing length theory, *Trans. Am. Soc. Mech. Engrs Ser. C* **85**, 137–152.

MALNES, D. 1966 Slip Ratios and Friction Factors in the Bubble Flow Regime in Vertical Tubes. *KR-110.*

NEAL, L. G. 1963 Local Parameters in Cocurrent Mercury–Nitrogen Flow. *ANL-6625.*

PETRICK, M. 1962 A Study of Vapor Carryunder and Associated Problems. *ANL-6581.*

ROUHANI, Z. 1974 Effect of Wall Friction and Vortex Generation on Radial Void Distribution—The Wall-Vortex Effect. *AE-497.*

SEKOGUCHI, K., FUKUI, H., TSUTSUI, M. & NISHIKAWA, K. 1972 A study of bubble statistics using an electrical resistivity probe. *Proc. 9th Jap. Heat Transfer Symp.* pp. 439–442.

TAMAO, S. 1970 Void Fractions in Mercury–Argon Two-Phase Flow. M.S. Thesis, Kyoto University.

VAN DEEMTER, J. J. & VAN DER LAAN, E. T. 1961 Momentum and energy balances for dispersed two-phase flow, *Appl. Sci. Res. Sec. A* **10**, 102–108.

VOHR, J. 1962 The energy equation for two-phase flow, *A.I.Ch.E. Jl* **8**, 280–281.

Auszug—Die Mikrostruktur einer vertikal aufwaertsgerichteten Zweiphasenstroemung von Luftblasen und Wasser, in einem vertikalen Rohr von 60 mm Durchmesser, wurde experimentell untersucht. Ueber den groessten Teil aller Querschnitte in voll ausgebildeter Zweiphasen-Blasenstroemung ergaben sich ziemlich flache radiale Profile der Phasen, der Blasen- und Wassergeschwindigkeiten, sowie des Verhaeltnisses der Phasengeschwindigkeiten, waehrend in Wandnaehe ein maximaler Blasenanteil zu beobachten war. Spektren der Blasen- und Wassergeschwindigkeiten zeigten beziehungsweise Poissonsche und Normalverteilung. Bei Versuchen mit konstanter Wassergeschwindigkeit sank die Turbulenzintensitaet mit wachsendem Gasdurchsatz zunaechst ab, um bei seiner weiteren Steigerung wieder zuzunehmen. Diese Erscheinung war umso ausgepraegter, je groesser die Wassergeschwindigkeit war.

Резтоме—Была экспериментально изучена микроструктура водо-воздушного двуфазного пузырькового течения, восходящего в вертикальной 60-тимиллиметровой круглой трубе и находящегося под атмосферным давлением. Результаты показывают, что в значительной части произвольного поперечного сечения потока скорости пузырьков и воды, как и отношение скоростей этих фае имеют вполне плоские радиальные профили, в то время как в пристеночной области наблюден максимум пустотной фракции. Спектры скоростей пузырьков и воды подчиняются распределению Пуассона и нормальному распределению соответственно. Эксперименты свидетельствуют, что степень турбулизации имеет тенденцию вначале понизиться с увеличением скорости тока газа при постоянстве скорости воды, а затем увеличиться при дальнейшем возрастании скорости газового тока. Это явление сказывается значительнее при более высоких скоростях воды.